

Quantifying plasmon resonance and interband transition contributions in photocatalysis of gold nanoparticle

Liang Dong(董亮), Chengyun Zhang(张成云), Lei Yan(严蕾), Baobao Zhang(张宝宝), Huan Chen(陈环), Xiaohu Mi(弥小虎), Zhengkun Fu(付正坤), Zhenglong Zhang(张正龙), and Hairong Zheng(郑海荣)

Citation: Chin. Phys. B, 2021, 30 (**7**): 077301. DOI: 10.1088/1674-1056/abfa0c
Journal homepage: http://cpb.iphy.ac.cn; http://iopscience.iop.org/cpb

What follows is a list of articles you may be interested in

Collective excitations and quantum size effects on the surfaces of Pb(111) films: An experimental study

Yade Wang(王亚德), Zijian Lin(林子荐), Siwei Xue(薛思玮), Jiade Li(李佳德), Yi Li(李毅), Xuetao Zhu(朱学涛), and Jiandong Guo(郭建东)

Chin. Phys. B, 2021, 30 (**7**): 077308. DOI: 10.1088/1674-1056/abfbcd

High sensitive chiral molecule detector based on the amplified lateral shift in Kretschmann configuration involving chiral TDBCs

Song Wang(王松), Qihui Ye(叶起惠), Xudong Chen(陈绪栋), Yanzhu Hu(胡燕祝), and Gang Song(宋钢)

Chin. Phys. B, 2021, 30 (**6**): 067301. DOI: 10.1088/1674-1056/abdda6

Enhanced circular dichroism of TDBC in a metallic hole array structure

Tiantian He(何田田), Qihui Ye(叶起惠), Gang Song(宋钢)

Chin. Phys. B, 2020, 29 (**9**): 097306. DOI: 10.1088/1674-1056/aba9ce

Quantization of electromagnetic modes and angular momentum on plasmonic nanowires

Guodong Zhu(朱国栋), Yangzhe Guo(郭杨喆), Bin Dong(董斌), Yurui Fang(方蔚瑞)

Chin. Phys. B, 2020, 29 (**8**): 087301. DOI: 10.1088/1674-1056/ab9698

Multiple Fano resonances in metal-insulator-metal waveguide with umbrella resonator coupled with metal baffle for refractive index sensing

Yun-Ping Qi(祁云平), Li-Yuan Wang(王力源), Yu Zhang(张宇), Ting Zhang(张婷), Bao-He Zhang(张宝和), Xiang-Yu Deng(邓翔宇), Xiang-Xian Wang(王向贤)

Chin. Phys. B, 2020, 29 (**6**): 067303. DOI: 10.1088/1674-1056/ab888c

---

Quantifying plasmon resonance and interband transition contributions in photocatalysis of gold nanoparticle*

Liang Dong(董亮), Chengyun Zhang(张成云), Lei Yan(严蕾)†, Baobao Zhang(张宝宝), Huan Chen(陈环), Xiaohu Mi(弥小虎), Zhengkun Fu(付正坤), Zhenglong Zhang(张正龙)‡, and Hairong Zheng(郑海荣)

School of Physics and Information Technology, Shaanxi Normal University, Xi'an 710062, *China*

(Received 19 January 2021; revised manuscript received 27 March 2021; accepted manuscript online 21 April 2021)

Localized surface plasmon has been extensively studied and used for the photocatalysis of various chemical reactions. However, the different contributions between plasmon resonance and interband transition in photocatalysis has not been well understood. Here, we study the photothermal and hot electrons effects for crystal transformation by combining controlled experiments with numerical simulations. By photo-excitation of $NaYF_4$:Eu^{3+}@Au composite structure, it is found that the plasmonic catalysis is much superior to that of interband transition in the experiments, owing to the hot electrons generated by plasmon decay more energetic to facilitate the reaction. We emphasize that the energy level of hot electrons plays an essential role for improving the photocatalytic activity. The results provide guidelines for improving the efficiency of plasmonic catalysis in future experimental design.

Keywords: surface plasmon, interband transition, hot electron, photothermal effect

PACS: 73.20.Mf, 31.15.xf **DOI:** 10.1088/1674-1056/abfa0c

Collective oscillation of conduction electrons in metal nanostructures, which is known as localized surface plasmon resonance (LSPR), has been widely studied in the past few decades due to their unique optical properties such as tunable resonance energy and enhanced optical absorption.[1] Various noble metal nanostructures such as Au nanoparticles (NPs), can be employed for such properties. LSPR can decay radiatively via photons or non-radiatively via excitation of hot electrons.[2] On the one hand, the hot electrons generated from plasmon decay can transfer to antibonding state of foreign molecules to catalyze the chemical reactions, which has been widely applied in water splitting,[3] dissociation of H_2,[4] and so on.[5,6] On the other hand, part of the hot electrons through the scattering between electrons and electrons and the scattering between electrons and phonons, eventually converts the absorbed photon energy into heat,[7] which is called the photothermal effect. Thermal energy is used to heat the particles themselves and the media environment surrounding the particles.[8] The heat loss from plasmon is previously considered an undesirable effect, until it is realized that LSPR can convert electromagnetic energy into thermal energy very efficiently on the nanoscale with great potentials in applications.[9] Furthermore, compared to a conventional heat source, the advantages of nanoparticles as heat sources include high local temperature and short thermal response time.[10] Therefore, the photothermal effects from LSPR is often used for photothermal therapy,[11] purifying sea water,[12] catalysis of the chemical reactions, and so on.[13]

When the wavelength of incident light is less than plasmon resonant wavelength, Au NPs also have strong intrinsic optical absorption due to interband transition.[14] Similar with the excitation of LSPR, the hot electrons excited by the interband transition can also convert the photon energy into heat energy through the non-radiative relaxation or transfer to molecules to catalyze the chemical reactions.[15,16] Zhou *et al.*[17] reported that hot electrons from both plasmon and interband transition could contribute to the hydrogen dissociation on aluminum nanocrystals. However, more details on the difference between plasmon and interband transition for photocatalysis are not clear even it is helpful for better understanding the atomic mechanism in photochemistry.

Here, the different contributions between plasmon resonance and interband transition in photocatalysis are investigated by combining finite element method[18] simulations with experiments. We analyze the photothermal effect and hot electrons for crystal transformation by photo-excitation of $NaYF_4$:Eu^{3+}@Au composite structure samples with different wavelength of the light. Transformation rate of plasmon-induced reaction is thousand times that of the interband transitions. We ascribe the main difference between the plasmon and interband transitions on the catalytic efficiency to the energy for hot electrons rather than the photothermal effect.

*Project supported by the National Key Research and Development Program of China (Grant No. 2020YFA0211300), the National Natural Science Foundation of China (Grant Nos. 92050112, 12074237, and 12004233), and the Fundamental Research Funds for Central Universities, China (Grant Nos. GK202103010 and GK202103018).

†Corresponding author. E-mail: yanlei@snnu.edu.cn

‡Corresponding author. E-mail: zlzhang@snnu.edu.cn

© 2021 Chinese Physical Society and IOP Publishing Ltd

These findings suggest that energetic hot electrons are crucial for achieving high efficiency in photocatalysis.

The numerical calculations were performed by finite element method with three-dimensional numerical simulation. In order to avoid the influence of reflection or scattering at the boundary on the calculation results, the perfectly matching layer (PML) was applied for the boundary. The medium environment around Au nanosphere was set to be air with refractive index $n = 1$. Considering that the laser spot used in the experiment is much larger than the diameter of gold nanospheres, the incident laser can be treated as a plane wave approximately, and the absorption cross section of gold nanosphere was calculated with the equation[19]

$$\sigma_{\text{abs}} = \frac{k}{\varepsilon_0 |E_0|^2} \int_{\text{NP}} \text{Im}(\varepsilon_\omega) |E_{(r)}|^2 \, \text{d}r, \tag{1}$$

where k is the wave vector, is the permittivity of the nanoparticle material, E_0 is the electric field amplitude of the incoming light considered as a plane wave, and $E_{(r)}$ is the total electric field amplitude.

We firstly investigate the photothermal effect of Au NPs in the visible range. The optical properties of Au NPs can be determined by LSPR and interband transition. LSPR for Au NPs is the collective oscillation of free electrons within the sp-band, while interband transition is essentially electrons transition from d-band to sp-band.[20] The optical response of the collection of free electrons can be described by a classical Drude model,[21] and that of electron transition from valence band to conduction band can be described by a similar Lorentz model.[22] The dielectric function is determined by Drude–Lorentz model[23]

$$\varepsilon = \varepsilon_{\text{Drude}} + \varepsilon_{\text{Lorentz}}. \tag{2}$$

Based on the heat diffusion equation, the temperature for the steady state of Au nanosphere is proportional to its absorption cross section,

$$\delta T_{\text{NP}} = \frac{Q}{4\pi\kappa R} = \frac{\sigma_{\text{abs}} I}{4\pi\kappa R}, \tag{3}$$

where κ is the thermal conductivity of the surrounding medium, R is the radius of the nanosphere, Q is the heat production power, and I is the power density of the incident light.

For the Au NPs with radius of 50 nm, the absorption cross sections were calculated by the above three models using finite element method. In Fig. 1(c) for Drude–Lorentz model, it is obvious that the absorption of gold nanosphere around 530 nm is mainly due to LSPR, and the absorption at wavelengths below 450 nm is mainly due to the interband transition according to the Drude model in Fig. 1(a) and Lorentz model in Fig. 1(b). Our calculation results are in accordance with the experiment data for gold film.[24] Optical absorption originating from interband transition is approximately 80% of the absorption from LSPR. Under the excitation of light with same power density, Au NPs at the plasmonic wavelength should show the better photothermal effect than that for interband transition if we assume Eq. (2) could well describe the temperature of NPs.

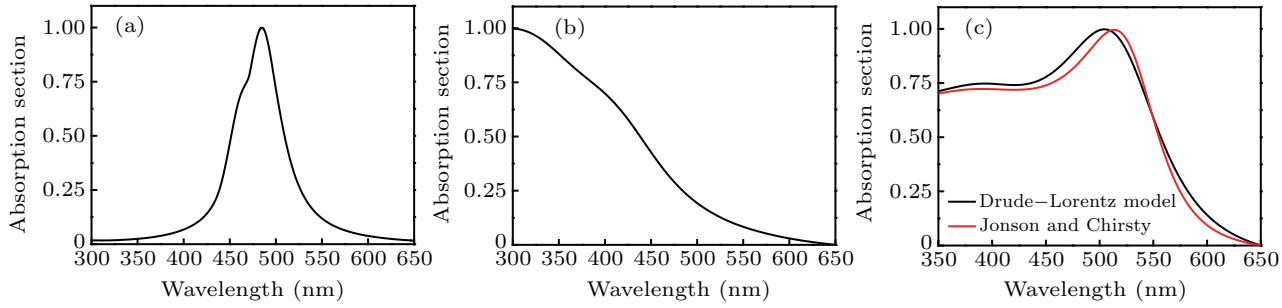


Fig. 1. Optical absorption of a gold nanosphere ($R = 50$ nm) immersed in air: (a) Drude model; (b) Lorentz model; (c) Drude–Lorentz model and experimentally measured gold film data.

The energy of hot electrons is an important factor for electron transfer-driven chemistry.[25] Next, we analyze the hot electron of Au NPs excited by the interband transition and plasmon decay. As shown in Fig. 2(a), the energy band for Au NP consists of two bands (d and sp), and intraband transitions (sp–sp) occur for LSPR. Since the electrons in the conduction band are excited and these electrons are usually located near the Fermi level, the energy of the hot electrons from plasmon decay can be considered close to the energy of the incident photon.[26] By comparison, in the photo-excitation of interband transition (d–sp), the energy of hot electrons greatly weakens by the existence of the band gap between d band and sp band.[27] Therefore, hot electrons from plasmon decay have higher energy than that from interband transitions in most cases.

The probability of hot electron generated from plasmon decay at a certain point is proportional to the square of the electric field strength at that point,[28] thus we integrate the square of plasmon-induced electric field over the volume V_{MFP}:

$$E^2_{\text{MFP}} = \frac{1}{V_{\text{MFP}}} \int |E_{(r)}|^2 \, \text{d}r, \tag{4}$$

where MFP is the mean free path of electron and taken as 25 nm for Au NPs here. Using this method, we calculated

the distribution of hot electrons in the gold nanosphere (R = 50 nm) with the varied wavelength of incident light. As shown in Fig. 2(b), the number of hot electrons by plasmon decay for gold nanosphere decreased rapidly on both sides of the peak around 530 nm.

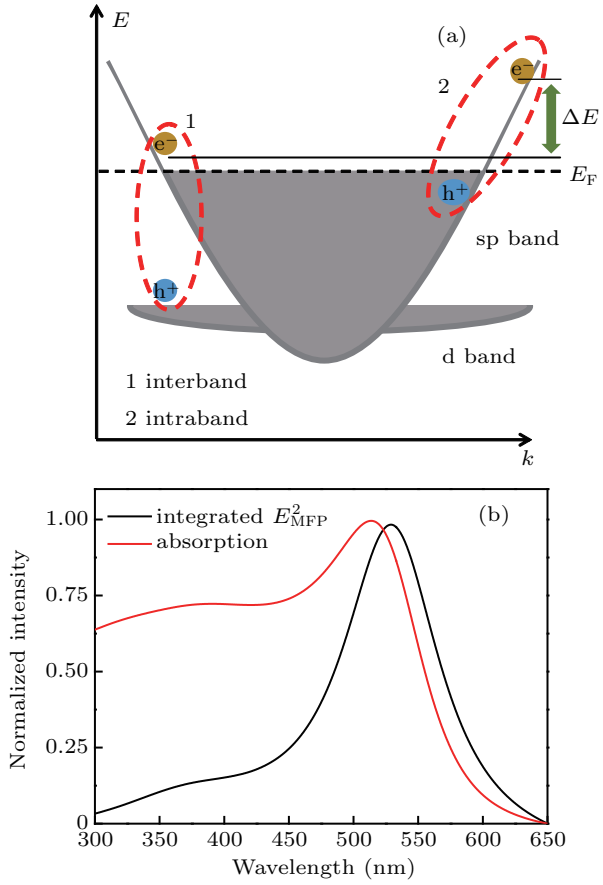


Fig. 2. (a) Schematic diagram of the hot electrons from interband transition and intraband transition. (b) The red line represents absorption cross section, and black line represents hot electrons related to intraband transition determined by the plasmon-induced local electric field. Both curves are normalized.

From the above discussion, both the photothermal and hot electrons effects for plasmon excitation are better than that for the interband transitions. In this sense, we estimate that the photocatalysis of plasmon is more effective than that of the interband transitions. In order to verify our prediction, we designed a catalytic experiment of the Au NPs attached to the $NaYF_4:Eu^{3+}$ nanoflower by laser irradiation.[29] $NaYF_4:Eu^{3+}$ nanoflowers with a size of about 500 nm were synthesized by coprecipitation method, and then gold nanoparticles with a radius of about 4 nm were attached to $NaYF_4:Eu^{3+}$ nanoflowers by wet chemical procedure. Compared to the instability of molecules at high temperature, the transformation of the crystal at high temperature is relatively stable. XRD patterns, absorption spectra, and TEM images of $NaYF_4:Eu^{3+}$@Au composite are in the supporting information.

As shown in Fig. 3(a), after the nanoflower irradiated by continuous lasers with different wavelengths in the same power (23 mW), both the $NaYF_4$ nanoflowers transform into single crystal Y_2O_3 due to the catalysis of Au NPs. This transformation can be clearly seen through the fluorescence spectrum of the product before and after the reaction. Under the irradiation of 442 nm corresponding to interband transition, the catalytic transformation takes 120 s. In contrast, under the irradiation of 532 nm corresponding to plasmon excitation, the catalytic transformation only takes 27 ms. We define the transformation rate as the inverse of time needed for transformation, and the details for transformation rate are in the supporting information. There is a huge difference in the transformation rate between the 442-nm and 532-nm excitations, and the ratio of transformation rate is more than 4000 times (Fig. 3(b)). In spite of our simple experimental approach, we find that plasmon-induced reaction is much more effective than interband transition, which may provide the support for similar catalysis experiments by selecting the appropriate excitation wavelength.

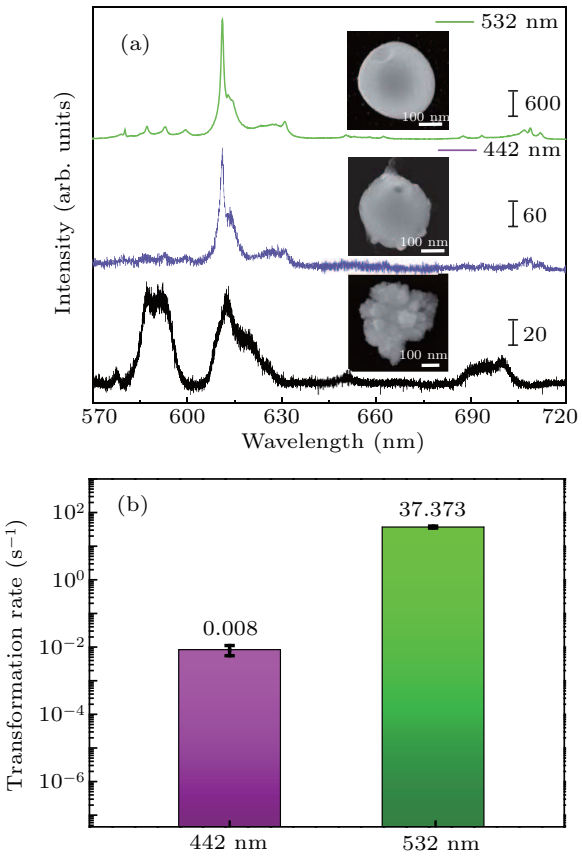


Fig. 3. (a) The black line represents the luminescence spectra of $NaYF_4:Eu^{3+}$ composite structure without any laser irradiation, and the purple and green lines represent *in situ* transformed $Y_2O_3:Eu^{3+}$ nanoparticle after laser irradiation with wavelengths of 442 nm and 532 nm, respectively. The insets show scanning electron microscope images of the corresponding particles after laser irradiation; (b) Transformation rate under different laser wavelengths.

To gain further insights into the photothermal catalysis and hot electrons catalysis, we studied the power dependence for photocatalysis under 532-nm laser excitation. As shown in Fig. 4, the transformation rate is linearly proportional to the laser power, implying a single-photon process.[30] In experi-

ments, this linear relationship has been observed for hydrogen dissociation on Au NPs[31] and ethylene epoxidation on Ag nanocubes.[32] The deviation from the linearity at the tail of the curve may be due to laser heating leading to the significant deformation or even fusion of Au NPs. In order to eliminate the effect of photothermal effect, we exclude the influence of the difference in absorption cross section between the two wavelengths of incident light on the steady-state temperature by reducing the laser power at 532 nm from 23 mW to 19 mW based on the data in Figs. 1 and 4.

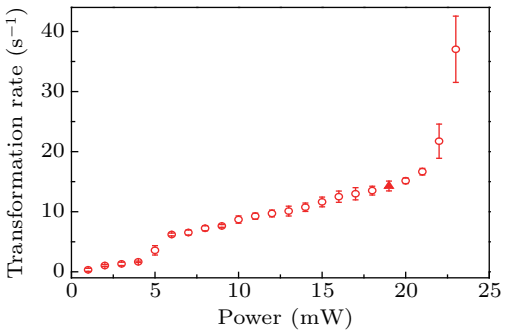


Fig. 4. Power-dependent transformation rate under continuous laser irradiation with the wavelength of 532 nm. The filled triangle symbol is the point we used to compare with the case of excitation wavelength of 442 nm.

Considering that the spot size used in the experiment is fixed, we simply consider the spot size to be 1 μm^2 to simplify the calculation. In this way, we can get the same value of heat production power Q as 0.36 mW for both excitation wavelengths of 442 nm and 532 nm based on Eq. (3) under the laser powers of 23 mW and 19 mW (the filled triangle symbol in Fig. 4), respectively. Specifically, based on $Q = \sigma_{abs} I$, σ_{abs} is taken as 0.016 μm^2 and 0.019 μm^2 according to optical absorption, and I is taken as 23 mW/μm^2 and 19 mW/μm^2 for the wavelengths of 442 nm and 532 nm, respectively. That is, heat production power for interband transitions and plasmon are almost same in this case. In contrast, the transformation rate of the sample under the laser of 532 nm is still 1700 times that of the transformation rate under the laser of 442 nm. This suggests that hot electrons mainly contribute to the catalysis in addition to thermal catalysis since redox reactions are involved. In our experiment, hot electrons may transfer to molecules on the surface of gold nanosphere. Specifically, the hot electrons can transfer to antibonding O–O state of molecular O_2 inducing the formation of ion,[33] and the reactive oxygen with higher utilization efficiency will facilitate the oxidization reaction of $NaYF_4$. Overall, hot electrons can promote the formation of and further promote the crystal transition of $NaYF_4$.

Next, we discuss the difference in hot electron catalysis between LSPR and interband transition for Au NPs. The lowest transition energy for the electron from the d band to the lowest energy of the sp band is 1.6 eV, and there still needs an additional 0.8 eV to reach the Fermi level.[34,35] So the electrons in the d band need at least 2.4 eV to reach the Fermi level.[36] Photon energy for the laser wavelength of 442 nm is about 2.8 eV. Therefore, the electrons in the d band can be excited at a maximum of 0.4 eV above the Fermi level for interband transition. However, the energy of this part of the electrons is too low to enter the antibonding state of molecular O_2. In this case, the hot electrons excited by the interband transition could not catalyze the transformation due to the low energy. Therefore, under the excitation of 442-nm laser, the photothermal effect of Au NPs dominates the reaction. In contrast, the photons of $\lambda = 532$ nm excite the electrons on the conduction band by plasmon excitation. Hot electrons exceed the Fermi level about 2.3 eV and still have enough energy to participate in the catalytic reaction. In this case, both photothermal effect and hot electrons from plasmon decay contribute to the catalysis. Hence, despite the photothermal effects of plasmon and interband transitions are almost same as discussed above, the effect of hot electrons determines the sharp difference of the transformation rate between the catalysis of plasmon and the interband transition.

In conclusion, the hot electrons and photothermal effects of Au NPs on catalysis of crystal transformation are investigated by combining theoretical calculations with experiments. The calculated results show that both the photothermal and hot electron effect of plasmon are better than that of interband transition for catalysis. In experiments, that transformation rate of plasmon-induced reaction is thousand times that of the interband transitions, owing to the difference of the energy for hot electron between interband transitions and plasmon. Hot electrons by plasmon decay are energetic enough to facilitate the reaction, while that from interband transition are energy deficiency. Photothermal effect dominates the interband-transition-induced reaction, while both hot electrons and photothermal effects contribute to the plasmon-induced reaction based on our analysis. Thereby, the energy of hot electrons generated in the process of photocatalysis is crucial for improving the catalytic rate, and the proper choice of the photon energy is an effective approach in manipulating chemical reactions.

Acknowledgement

The authors thank Prof. Jiangbo Lu (Shaanxi Normal University) for the sample characterization by FEI Titan cubed Themis G2 300 microscope.

References

[1] Pelton M, Aizpurua J and Bryant G 2008 *Laser Photon. Rev.* **2** 136
[2] Sönnichsen C, Franzl T, Wilk T, von Plessen G, Feldmann J, Wilson O and Mulvaney P 2002 *Phys. Rev. Lett.* **88** 077402
[3] Mascaretti L, Dutta A, Kment Š, Shalaev, V M, Boltasseva A, Zbořil R and Naldoni A 2019 *Adv. Mater.* **31** 1805513

[4] Guselnikova O, Trelin A, Miliutina E, Elashnikov R and Lyutakov O 2020 *ACS Appl. Mater. Interfaces* **12** 28110
[5] Xiao M, Jiang R, Wang F, Fang C, Wang J and Yu J C 2013 *J. Mater. Chem. A* **1** 5790
[6] Tu H, Cheng J, Pan G, Han L, Duan B, Wang H, Chen Q, Xu S, Dai Z and Pan L 2021 *Chin. Phys. B* **30** 027802
[7] Park S, Pelton M, Liu M, Guyot-Sionnest P and Scherer N F 2007 *J. Phys. Chem. C* **111** 116
[8] Kim M, Lee J and Nam J 2019 *Adv. Sci.* **6** 1900471
[9] Chen X, Chen Y, Yan M and Qiu M 2012 *ACS Nano* **6** 2550
[10] Baffou G and Quidant R 2013 *Laser Photon. Rev.* **7** 171
[11] Gobin A M, Lee M H, Halas N J, James W D, Drezek R A and West J L 2007 *Nano Lett.* **7** 1929
[12] Zhou L, Tan Y, Wang J, Xu W, Yuan Y, Cai W, Zhu S and Zhu J 2016 *Nat. Photon.* **10** 393
[13] Zhan C, Moskovits M and Tian Z Q 2020 *Matter* **3** 42
[14] Fan X, Zheng W and Singh D J 2014 *Light: Sci. Appl.* **3** e179
[15] Minutella E, Schulz F and Lange H 2017 *J. Phys. Chem. Lett.* **8** 4925
[16] Harutyunyan H, Martinson A, Rosenmann D, Khorashad L K, Besteiro L V, Govorov A O and Wiederrecht G P 2015 *Nat. Nanotechnol.* **10** 770
[17] Zhou L, Zhang C, McClain M J, Manjavacas A, Krauter C M, Tian S, Berg F, Everitt H O, Carter E A, Nordlander P and Halas N J 2016 *Nano Lett.* **16** 1478
[18] Bathe K 2000 *Finite Element Method* (John Wiley & Sons, Inc.)
[19] Baffou G, Quidant R and Girard C 2009 *Appl. Phys. Lett.* **94** 153109
[20] Werner D, Hashimoto S and Uwada T 2010 *Langmuir* **26** 9956
[21] Vial A, Grimault A S, Macias D, Barchiesi D and Chapelle M 2005 *Phys. Rev. B* **71** 85416
[22] Pakizeh T 2011 *J. Phys. Chem. C* **115** 21826
[23] Rakić A D, Djurišić A B, Elazar J M and Majewski M L 1998 *Appl. Opt.* **37** 5271
[24] Johnson P B and Christy R W 1972 *Phys. Rev. B* **6** 4370
[25] Schlather A E, Manjavacas A, Lauchner A, Marangoni V S and Halas N J 2017 *J. Phys. Chem. Lett.* **8** 2060
[26] Khurgin J B and Boltasseva A 2012 *MRS Bull.* **37** 768
[27] Ortolani M, Mancini A, Budweg A, Garoli D, Brida D and Angelis F D 2019 *Phys. Rev. B* **99** 035435
[28] Zhao H, Zheng B Y, Manjavacas A, Mcclain M, Nordlander P and Halas N J 2015 *Nat. Commun.* **6** 7797
[29] Zhang C, Kong T, Fu Z, Zhang Z and Zheng H 2020 *Small* **12** 8768
[30] Kale M J, Avanesian T and Christopher P 2014 *ACS Catal.* **4** 116
[31] Mukherjee S, Libisch F, Large N, Neumann O and Halas N J 2012 *Nano Lett.* **13** 240
[32] Christopher P, Xin H, Marimuthu A and Linic S 2012 *Nat. Mater.* **11** 1044
[33] Christopher P, Xin H and Linic S 2011 *Nat. Chem.* **3** 467
[34] Christensen N E and Seraphin B O 1971 *Solid State Commun.* **8** 1221
[35] Hirohito F 1971 *J. Phys. Soc. Jpn.* **30** 399
[36] Berciaud S, Cognet L, Tamarat P and Lounis B 2005 *Nano Lett.* **5** 515